Collective stabilization of hydrogen chemisorption on graphenic surfaces

Dragan Stojkovic, Peihong Zhang, Paul E. Lammert, and Vincent H. Crespi
Department of Physics, Materials Research Institute, 104 Davey Laboratory, Penn State University, University Park, Pennsylvania 16802-6300, USA

(Received 13 June 2003; revised manuscript received 20 August 2003; published 14 November 2003)

A graphene sheet is well known to be highly stable against chemisorption of a single hydrogen atom, since a puckered sp^3 hybridized site heavily distorts the surrounding sp^2 framework. However, successive adjacent chemisorbed hydrogen atoms can engage in a collective stabilization mediated by cooperative alternate puckering in the underlying carbon sheet. After several chemisorbed atoms, the binding energy for further adsorption changes sign and becomes favorable. This process requires access to both sides of the graphene sheet. Therefore it is suppressed on a graphite surface, but may be accessible in carbon nanotubes, if the initial kinetic barrier to creating the nucleation island can be overcome.

DOI: 10.1103/PhysRevB.68.195406 PACS number(s): 68.43.Bc, 68.43.Fg, 61.46.+w

I. INTRODUCTION

The similar energies of different hybridized states of carbon lead to its versatile chemical behavior. Graphite and nanotubes, as two elemental forms of carbon, demonstrate this flexibility through their ability to make new chemical bonds with chemisorbed atoms while preserving the original carbon hexagonal net. One important case in which this happens is hydrogen chemisorption;[1–7] here we focus on the strong variations of the energy of chemisorption as a function of the hydrogen coverage.

Although catalysts such as Pt on graphite can dissociate H_2 molecules and place atomic hydrogen in contact with graphite, a defect-free graphene basal plane is highly resistant to chemical attack by free hydrogen atoms. Not only is the kinetic barrier to hydrogen chemisorption generally large, but an isolated hydrogen atom sp^3 bonded to a graphene plane is also energetically unfavorable compared to the clean graphene sheet plus the same hydrogen in the (molecular) gas phase.[3] However, the binding of an isolated hydrogen atom onto a clean and defect-free graphite basal plane does not provide a complete picture of the pathways towards a fully hydrogenated carbon sheet. An sp^3 coordinated carbon atom within a graphene layer imposes a strong pattern of buckling on the surrounding atoms; the buckling patterns from nearby sp^3 atoms can overlap and possibly reinforce. Such a collective stabilization, favoring successive hydrogen addition, is distinct from the well-known effects of broken aromaticity in hydrogenating small molecules. For example, in the conversion of benzene to cyclohexane, the first hydrogen attachment is most costly, since it breaks the π ring conjugation; later hydrogens are easier to attach. In a small molecule like benzene, the bond angles can adjust relatively freely to accommodate nearby sp^2 and sp^3 atoms. In contrast, an extended graphene sheet imposes strong elastic constraints that create a frustrated sp^3-like buckling around a single chemisorbed hydrogen. However, if chemical attachment is possible on both sides of the graphene layer, then these local bucklings can reinforce each other. This cooperative sheet-mediated absorbate-adsorbate interaction can change the sign of the adsorption energetics, making further chemisorption energetically favorable. For comparison, note that graphite surface has been flourinated, converting the sp^2 network largely to sp^3, since the F_2 molecule is highly reactive.[4,8–10]

II. METHODOLOGY

Unlike hydrogen physisorption, which involves subtle many-body van der Waals effects,[11] hydrogen chemisorption can be well described by standard semiempirical and density-functional methods. However, in order to accurately describe collective effects, large systems must be simulated. Therefore we first employ a focused set of density-functional theory (DFT) calculations to validate further use of more computationally efficient empirical tight-binding total-energy methods[12] for a much larger set of complex multiadsorbate geometries.

The total energies for each configuration with chemisorbed hydrogen are compared to those of a suitable reference structure, namely a pure-carbon pure-sp^2 structure plus the same hydrogen atoms in isolated hydrogen molecules:

$$\Delta E = E - E_0 - \frac{N_H}{2} E_{H_2}, \tag{1}$$

where N_H is the number of attached hydrogens, E is the total energy of the configuration in question, E_0 is the energy of the pristine pure-sp^2 pure-carbon system and E_{H_2} is the energy of a single hydrogen molecule. Negative ΔE corresponds to energetically favorable adsorption. It can be divided by N_H to obtain a binding energy per hydrogen atom. Vibrational entropy will favor hydrogen geometries with weaker bonds, but this effect should not disrupt the overall energetic trend towards cooperative adsorption. Since we focus on relative energetics, we do not consider vibrational entropies or pressure-dependent gas-phase entropic terms. This treatment differs from previous studies,[5] in that we compare the bound system to a clean substrate plus molecular rather than atomic hydrogen.

An isolated chemisorbed hydrogen induces a local distortion of the surrounding carbon atoms, creating an intermediate sp^2/sp^3 bonding character on neighboring atoms. This distortion induces a slight dangling-bond character in its im-

mediate neighborhood and affects the energetics and kinetics for adsorption of additional hydrogen. The most favorable site for successive hydrogen addition should generally be immediately adjacent to the existing cluster, at the point with maximal bonding distortion. The number of possible arrangements of nearby adsorbed hydrogens grows roughly exponentially as the number of hydrogen atoms increases. Therefore instead of exhaustively analyzing all possible configurations for a given N_H, we start from $N_H=1$ and construct successively larger clusters by following the lowest-energy pathway for successive hydrogen addition. For small or linear clusters this strategy requires evaluation of $\sim N_H$ structures, since roughly half of the possible cluster edge sites are equivalent. For big compact clusters, evaluation of $\sim\sqrt{N_H}$ structures is enough at each stage, since every site near the perimeter of the N_H configuration must be tested to determine the most favorable N_H+1 configuration.

We examine three different stages with successively higher hydrogen densities: (i) the beginnings of chemisorption, wherein a small number of hydrogen atoms attach to a graphene surface in a local cluster, (ii) the extension of an adsorbed state along a tube axis, using high-symmetry configurations to simplify interpretation and (iii) the hydrogenation of the last few remaining sp^2 carbon atoms in an almost fully hydrogenated sheetlike carbon structure.

A. Computational technique

To examine the initiation of chemisorption onto an (8,8) carbon nanotube, we use the VASP (Ref. 13) package to make a series of local-density approximation (LDA) density-functional theory (DFT) calculations with ultrasoft pseudopotentials and a 300-eV plane-wave energy cutoff. We use a supercell containing three unit cells of the (8,8) tube (with total 96 carbon atoms) to adequately isolate the clusters of attached hydrogens in each repeated unit. Since the chemisorbed patches are well separated and we calculate in a threefold supercell, the simulations use only the Γ ($\vec{k}=0$) point. The supercell has dimensions of 21 Å $\times$ 21 Å $\times a_z$, where $a_z\approx$ 7.3 Å varies between structures, since the system is fully relaxed along the z direction. The ionic relaxation has been carried on up to the point when the relative total energy change is less than 1×10^{-4} per unit cell. The tight-binding calculations for the same supercell structures have been made within a nonorthogonal tight-binding scheme[12] implemented in program Trocadero.[14] In this calculation a structure has been considered relaxed when the relative total energy change becomes lower than 2×10^{-5}. In every case, the structure is fully relaxed into the local energetic minimum.

III. RESULTS

A. Beginning of chemisorption

Figure 1 shows relative total energies ΔE for a growing hydrogen cluster with atoms attached to both sides of an (8,8) nanotube, calculated using spin polarized LDA DFT. The smallest chemisorbed clusters are unstable, but at $N_H=4$ the chemisorbed state becomes energetically favorable. This behavior manifests as a collective reinforcement of the buckled sp^3 network. As a consequence of the wall curvature, the cluster grows further with hydrogen arranged in an armchair circumferential row, with more hydrogens on the outside surface than on the inside surface (Figs. 3 and 4).

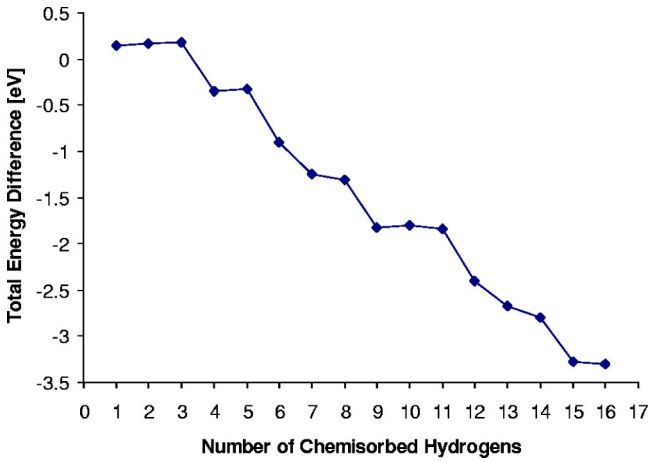

FIG. 1. LDA DFT results for the energy ΔE of the hydrogen chemisorption on the (8,8) tube, following the minimal energy path described in the main text.

Unlike most chemisorbed or physisorbed systems, which have a relatively weak density-dependent binding energy, the binding energy for hydrogen chemisorption in this case is highly density-dependent and even changes sign. The explanation for this distinction is twofold. First, carbon is nearly isoenergetic in two very different bonding geometries, so that the chemisorption process is accompanied by a large change in local bond angles. Second, the graphene substrate is a single two-dimensional atomic layer, rather than the surface of a three-dimensional solid. This very thin substrate is then susceptible to buckling distortions perpendicular to the plane and, unlike bulk graphite, atoms can attach to both sides.

If collective effects were not important, then the binding energy ΔE_H per hydrogen atom would be a constant and the energy gain for N_H adsorbed hydrogens would be a straight line intersecting the origin: $E_H=\Delta E_H N_H$. The curve in Fig. 1 clearly does not have this form and even changes sign at $N_H=4$. In the limit of large N_H the curve becomes roughly linear, showing that the collective stabilization of chemisorbed hydrogens is relatevely short ranged.

Next we calculate the same series of structures using the tight-binding total-energy approximation. The result (black diamonds on Fig. 2) shows the same trend as the DFT result (Fig. 1), but shifted upwards and with a somewhat smaller slope (possibly due to an underestimate of longer-range contributions from broken aromaticity). Both curves have peaks and valleys with similar locations, except at the beginning of the chemisorption process, where tight binding overestimates the graphene resistance to the first hydrogenization and shows a rather slow change in the cluster stability, predicting the first stable cluster only after nine hydrogens. In addition, the tight-binding-based minimal energy sequence yields the same shape for the optimal 16-atom hydrogen cluster: an armchair row around the tube. This comparison shows that the tight-binding total-energy method is reasonably accurate for carbon in the vicinity of sp^2 and sp^3 bonding geometries

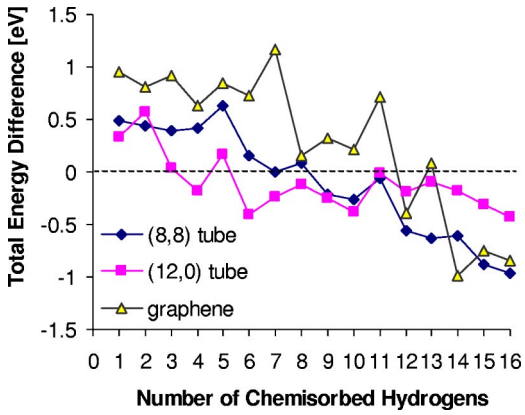

FIG. 2. (Color online) Tight-binding total-energy difference ΔE of hydrogen chemisorption following the minimal energy path, as described in the main text. Configurations with negative ΔE are more stable than a corresponding clear carbon structure plus molecular hydrogen.

and so should be able to describe the main features of cooperative interactions between nearby adsorbates.

Since tight binding gives the correct trend for the total energy of hydrogen chemisorption, we next use it in a comparative study of hydrogen chemisorption onto three different systems: the tripled unit cell (8,8) nanotube already mentioned, a doubled unit cell (12,0) tube, also with 96 carbon atoms, and a flat defect-free single graphene sheet with 384 carbon atoms (but roughly the same unit-cell volume as for the tubes). The flat graphene sheet, when compared to the tube systems, reveals the effects of wall curvature and bond orientation relative to the principal axes of curvature. In each case, we assume that atomic hydrogen has access to both sides of the carbon surface, as would be the case for a nanotube with open ends or sidewalls.[15]

Figure 2 shows the tight-binding energies ΔE for growing clusters. The smallest chemisorbed clusters are again unfavorable, but at $N_H \approx 6-10$ the chemisorbed state becomes energetically favorable in all three structures. The minimal stable cluster is smaller when the curvature of the underlying carbon net is bigger, since sp^3 bonding angles for outwardly attached atoms are more easily fit onto a curved surface and the system can adjust the relative numbers of inside and outside hydrogen atoms.

In each case, the patches of hydrogen are most stable as a double row of adsorbed atoms[7] (see Figs. 3 and 4). For the flat sheet, this double row follows the so-called zigzag direction of the graphene lattice. As a consequence of wall curvature, both nanotubes favor hydrogen arranged along a circumferential path, even though the $(n,0)$ and (n,n) tubes have quite different bond orientations relative to the tube axis.[16] The small diameter of the (12,0) tube cannot easily support an sp^3 state with equal numbers of hydrogens on the outside and inside: the inside hydrogens are less compatible with the overall wall curvature. Therefore a second row starts before the first row is complete, similar to what happens for intermediate sized pure-sp^3 tubes.[17] For larger radii the curvature is less important and hydrogen atoms can complete a ring before the next row begins.

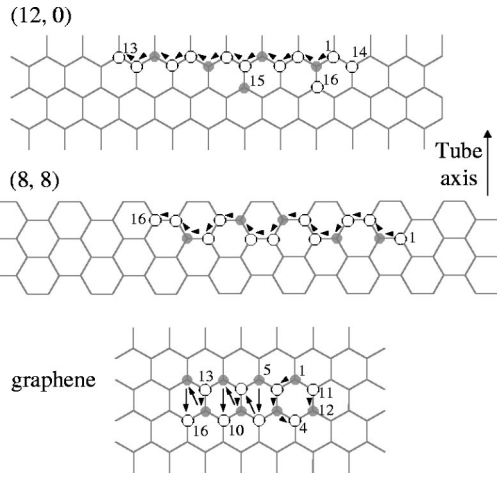

FIG. 3. Sequences of hydrogen atoms chemisorbed by following a minimal energy path for the (8,8) and (12,0) tubes and graphene. Gray disks represent atoms chemisorbed inside the tube or below the sheet. Arrows show the path of successive hydrogen addition. Hydrogen atoms with explicit index numbers are discontinuities in the path.

B. Propagation of chemisorption

The above results suggest that progressive hydrogenation would proceed in a row by row fashion, as has been found experimentally for fluorinated systems.[8] Verifying this model in detail is not a simple task, since cluster formation becomes harder to follow step by step as the number of hydrogen atoms increases. Instead, we model further growth by restricting attention to a set of high-symmetry structures with hydrogen atoms arranged in a series of rings around the (8,8) and the (12,0) tubes. The small clusters already show that not all hydrogen atoms in one row should be on the same side of the tube, so these structures are not energetically the most

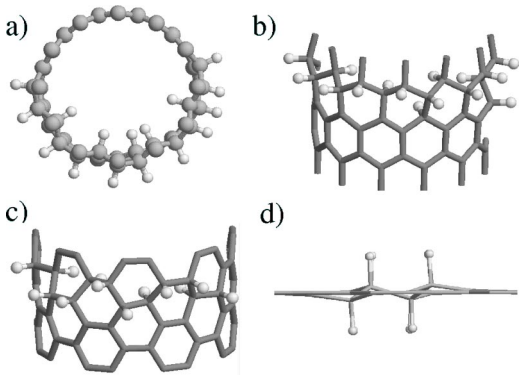

FIG. 4. The final configurations of a sequence of hydrogen atoms chemisorbed by following a minimal energy path. (a) On the smaller-diameter (12,0) tube, the strain on the clear part of the tube induces a new row [(b), side view] to start before the first row circuits the belly of the tube. (c) In the (8,8) tube, the cluster again grows as a ring around the circumference. (d) In the graphene sheet, hydrogen atoms arrange in a double zigzag row. The edge-on view for the graphene sheet emphasizes the sp^3-like vertical distortions away from the perfectly planar sp^2 starting structure. Schematic top views of the same structures are shown in Fig. 3.

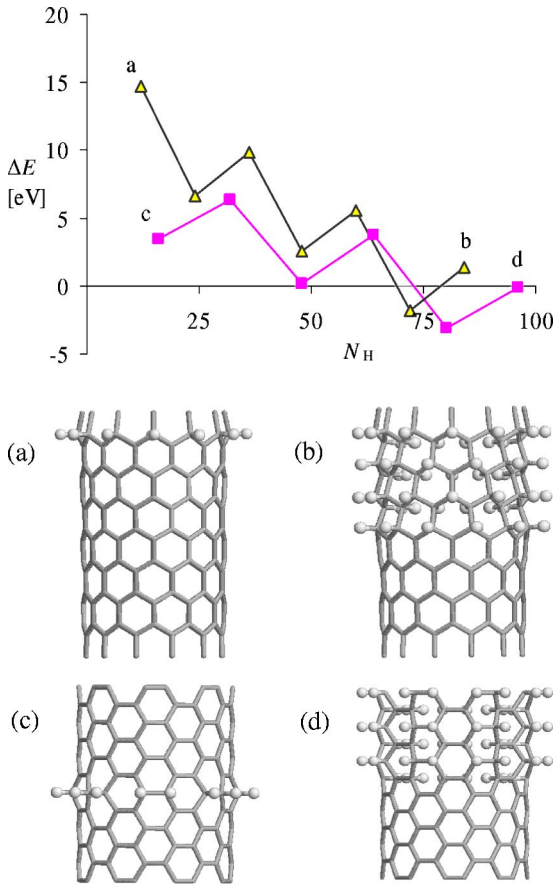

FIG. 5. (Color online) Difference in the energies ΔE for (8,8) (squares) and (12,0) (triangles) tubes with completed rows of chemisorbed hydrogen. Rows alternate from the outside to the inside of the tube. Four structures [(a)–(d)] are detailed in the text.

favorable, but they provide a simple view of possible modes of propagation for an adsorption front along the axis of the tube.

Figure 5 shows the energy difference ΔE for successive row-by-row adsorption. In order to avoid interaction between images, these tight-binding calculations use larger supercells with 192 carbon atoms. The outside (represented in the text as $\uparrow$) and inside ($\downarrow$) hydrogen rings alternate, following by the unhydrogenated ($-$) carbon sp^2 rings. Since the atoms in each ring are equivalent, corresponding structures can be labeled using their cross sectional shape. The figure contains models for the first configuration, ($\uparrow-----------$), containing just one hydrogen row attached on the outside surface and two later configurations: ($\uparrow\downarrow\uparrow\downarrow\uparrow\downarrow----$) for the (8,8) tube (with six filled rows) and ($\uparrow\downarrow\uparrow\downarrow\uparrow\downarrow\uparrow-----$) for (12,0) tube (with seven filled rows).

Energies for the higher-symmetry row-by-row filling are higher than those for the small clusters, as expected. The axial propagation of the chemisorbed state favors addition of rows in pairs, rather than sequentially row by row, since the distortion of the remaining sp^2 part is then minimized and the sp^3 atoms interior to the patch maintain a consistent geometry. The reduction in the total energy per hydrogen atom after each ($\uparrow\downarrow$) step is $\Delta E/N_H \approx -100$ meV for the (8,8) tube and $\Delta E/N_H \approx -180$ meV for the (12,0) tube. Similar to the initiation of chemisorbtion, the total energy ΔE decreases and the overall process is self-propagating in an energetic sense. As a consequence of different carbon bond orientations, the armchair (8,8) tube prefers configurations with one extra row on the outside, while the zigzag (12,0) tube prefers equal numbers of inside and outside rows. In larger systems, antiphase boundaries between different domains could introduce frustration into the pattern of buckling at the boundaries.

C. CH sp^3 tubes

Finally we consider the other extreme of hydrogen chemisorption, a tube completely filled with hydrogen. This is a complement to the clean tube, being again a uniform tubular structure, but built with sp^3 instead of sp^2 carbon. For each sp^2 tube there is its sp^3 carbon-hydrogen counterpart.[17] These structures are significantly more stable than their sp^2 twins (plus gaseous hydrogen). For example, the (8,8) sp^3 tube is 140 meV per hydrogen atom more stable than its sp^2 counterpart, while the (12,0) tube is preferred by 233 meV per hydrogen. The final steps of adsorption just before attaining complete sp^3 coverage perhaps most strongly demonstrate the importance of the collective stabilization. It is simplest to examine this limit by working backwards and considering the removal of a succession of hydrogen atoms from a saturated tube. The sp^3 (8,8) tube with 96 carbon atoms and a single missing hydrogen atom (assumed to form half of an H_2 molecule) is already $\sim$1.9 eV (in the tight binding) less stable than the saturated tube. Therefore the reverse reaction, i.e., the completion of saturation, is highly favorable. The second and third hydrogen atom can be detached from nearby sites in a several different ways, but they all have similar total energy cost of about $\sim$1.5 eV, within the same empirical approximation.

IV. CONCLUSIONS

The resistance of a pristine graphite basal plane to attack by atomic hydrogen has two distinct kinetic barriers: the familiar ''local'' barrier against changing the bond hybridization of a specific carbon atom and also a more collective ''global'' nucleation barrier, wherein a finite number of adjacent hydrogens must be attached before the addition of subsequent hydrogens becomes energetically favorable. The kinetic barrier against this self-reinforcing process is substantial. Methods to overcome this nucleation barrier could include the creation of defects in the sp^2 sheet, the incorporation of pre-configured small hydrocarbons that build in the structure of a seed cluster, or initial fluorination of the sheet, followed by a concerted exchange of fluorine for hydrogen. Single-walled carbon nanotubes seem a particularly favorable substrate for this behavior, since both sides of the sp^2 surface are potentially accessible and the wall curvature reduces the size of the critical cluster. One possible source of the atomic hydrogen needed is a dispersion of nanoparticulate Pt catalyst. The local kinetic barrier

against chemisorption is much smaller for atomic hydrogen (0.3 eV) than for molecular hydrogen (around 3 eV).[18] This barrier may decrease further with progressive buckling of the carbon surface, since potential host carbons adjacent to the current cluster deviate more strongly towards an incipient sp^3 dangling bond structure under the influence of the collective sheet distortions. Regardless, kinetic barriers are likely to remain significant.

In summary, we simulated the chemisorption of hydrogen on carbon surfaces, allowing hydrogen to access both sides, using DFT and semiempirical tight-binding methods. We check the tight-binding results against DFT in one system and then use tight binding as more efficient method to investigate hydrogen chemisorption on zigzag and armchair tubes and the graphene sheet. In each of these cases the hydrogen cluster becomes favorable after exceeding some threshold size. On tubes hydrogen clusters prefer to grow as a belt, in a row-by-row manner, so we model the cluster's further extension by examing a series of well ordered structures, with hydrogen atoms arranged in rows around the tube. This system gains energy if the rows are added in pairs, one on the inside and one on the outside of the tube. Next, we discuss the other end of the chemisorption process, fully sp^3-bonded CH tubes and find them to be very stable structures. Finally, we discuss possible experimental realizations of the modeled systems and propose methods to help overcome the cluster nucleation barrier.

ACKNOWLEDGMENTS

This research has been supported by the National Science Foundation through Grant Nos. DMR-9876232 and NIRT DMR-0103585 and the Army Research Office through Grant No. DAAD19-99-1-0167. We acknowledge the National Partnership for Advanced Computational Infrastructure.

[1] G. E. Froudakis, J. Phys.: Condens. Matter **14**, R453 (2002).
[2] L. Jeloaica and V. Sidis, Chem. Phys. Lett. **300**, 157 (1999).
[3] X. Sha and B. Jackson, Surf. Sci. **496**, 318 (2002).
[4] C. W. Bauschlicher, Jr., Chem. Phys. Lett. **322**, 237 (2000); Nano Lett. **1**, 223 (2001).
[5] O. Gülseren, T. Yildirim, and S. Ciraci, Phys. Rev. B **66**, 121401 (2002); T. Yildirim, O. Gülseren, and S. Ciraci, *ibid.* **64**, 075404 (2001).
[6] S. M. Lee, K. H. An, Y. H. Lee, G. Seifert, and T. Frauenheim, J. Am. Chem. Soc. **123**, 5059 (2001).
[7] G. E. Froudakis, Nano Lett. **1**, 179 (2001).
[8] K. F. Kelly, I. W. Chiang, E. T. Mickelson, R. H. Hauge, J. L. Margrave, X. Wang, G. E. Scuseria, C. Radloff, and N. J. Halas, Chem. Phys. Lett. **313**, 445 (1999).
[9] E. T. Mickelson, C. B. Huffman, A. G. Rinzler, R. E. Smalley, R. H. Hauge, and J. L. Margrave, Chem. Phys. Lett. **298**, 188 (1998); P. J. Boul, J. Liu, E. T. Mickelson, C. B. Huffman, L. M. Ericson, I. W. Chiang, K. A. Smith, D. T. Colbert, R. H. Hauge, J. L. Margrave, and R. E. Smalley, *ibid.* **310**, 367 (1999).
[10] T. Mallouk, B. L. Hawkins, M. P. Conrad, K. Zilm, G. E. Maciel, and N. Bartlett, Philos. Trans. R. Soc. London, Ser. A **314**, 179 (1985).
[11] B. K. Pradhan, A. R. Harutyunyan, D. Stojkovic, J. C. Grossman, P. Zhang, M. W. Cole, V. Crespi, H. Goto, J. Fujiwara, and P. C. Eklund, J. Mater. Res. **17**, 2209 (2002).
[12] D. Porezag, Th. Frauenheim, Th. Kohler, G. Seifert, and R. Kaschner, Phys. Rev. B **51**, 12947 (1995); A. P. Horsfield, *ibid.* **56**, 6594 (1997).
[13] G. Kresse and J. Hafner, Phys. Rev. B **47**, 558 (1993); G. Kresse and J. Furthmuller, Comput. Mater. Sci. **6**, 15 (1996).
[14] E. Hernández, C. Goze, P. Bernier, and A. Rubio, Phys. Rev. Lett. **80**, 4502 (1998).
[15] P. M. Ajayan, T. W. Ebbesen, T. Ichihashi, S. Iijima, K. Tanigaki, and H. Hiura, Nature (London) **362**, 522 (1993); M. S. C. Mazzoni, H. Chacham, P. Ordejon, D. Sanchez-Portal, J. M. Soler, and E. Artacho, Phys. Rev. B **60**, R2208 (1999).
[16] The use of periodic boundary conditions, which constrain the tube to be straight, may affect the preference for a circumferential path.
[17] D. Stojkovic, P. Zhang, and V. H. Crespi, Phys. Rev. Lett. **87**, 125502 (2001).
[18] E.-C. Lee, Y.-S. Kim, Y.-G. Jin, and K. J. Chang, Phys. Rev. B **66**, 073415 (2002).